

With a little help of DNA: Morphological diversity of colloidal self-assembly

Alexei V. Tkachenko

Bell Labs, Lucent Technologies, 600-700 Mountain Ave., Rm 1D329, Murray Hill, NJ 07974

E-mail: alexei@bell-labs.com

We study theoretically a binary system in which an attraction of unlike particles is combined with a type-independent soft core repulsion. The possible experimental implementation of the system is a mixture of DNA-covered colloids, in which both the repulsion and the attraction may be induced by DNA solution. The system is shown to exhibit surprisingly diverse and unusual morphologies. Among them are the diamond lattice and the membrane phase with in-plane square order, a striking example of *spontaneous compactification*.

PACS numbers: 82.70.Dd, 81.16.Dn, 87.14.Gg, 42.70.Qs

Self-assembly in colloidal systems has attracted a lot of interest as an experimental tool for study of crystallization and glassiness [1]. It also has a great potential for the submicron technology, especially for fabrication of photonic band gap materials [2]. The progress in these directions is considerably limited by the lack of diversity of the crystalline morphologies achievable by self-assembly. Typically, a monodisperse colloidal system crystallizes into a close-packed structure (FCC, or another stacking of hexagonal layers) [1], [3].

In this paper, we propose a system which combines relatively simple interactions with a rich and unexpected phase behavior. It is inspired by recent experimental demonstration of DNA-assisted self-assembly of nanoparticles [4,5]. The key elements of that scheme are submicron spheres (e.g. golden, silica, or other) covered with short single-stranded DNA “markers”. The marker sequence determines the particle type (there may be many markers per particle, but their sequences must be the same). One can now introduce type-dependent interactions between the particles by adding “linker” DNA molecules, whose ends are complementary to the corresponding markers. These interactions are very selective, reversible and tunable.

We start our discussion with a generic model in which the physical origin and details of the inter-particle interactions are largely ignored. Let us consider a binary system of spheres, of the same diameter d , repelling each other with a soft-core potential, $U(r)$. In addition, the unlike particles may stick to each other with binding energy $-E$. We will study the phase behavior of the system for various values of two parameters: the aspect ratio, d/ξ (ξ is the range of potential $U(r)$), and the relative strength of the attraction, E/U_0 (here $U_0 \equiv U(d)$). Later in the paper, we discuss how this system can be implemented experimentally. Our specific proposal is to use DNA to introduce type-dependent attraction, and polymeric (possibly, also DNA) brush to induce the repulsive

potential.

The non-trivial phase behavior of the discussed system is a result of interplay between the adhesive energy and the soft-core repulsion. We will consider only structures with 1 : 1 composition. Let r_k be a distance to the k -th nearest neighbor of a particle in a given structure ($r_1 \equiv d$), let Z_k be the average number of such neighbors, and Z be the average number of cohesive contacts per particle (coordination number). If the entropic effects are neglected, the energy per particle (i.e. the average chemical potential of A and B particles) is

$$\mu = \frac{1}{2} \left(-ZE + \sum_{k=2}^{\infty} Z_k U(r_k) \right) \simeq \frac{1}{2} (-ZE + Z_2 U(r_2)) \quad (1)$$

Here, we have neglected the contribution from the particles beyond the second nearest neighbors, which is a reasonable approximation for $d/\xi \gg 1$. In order to assure its validity, we perform a posteriori check of the effect of the higher order corrections on our results. It is straightforward to use the above equation to identify the phase boundary between two different structures. Since the chemical potential should be continuous at the transition, one can express the critical value of adhesive energy E in terms of the geometrical parameters (Z , Z_2 , and r_2) of the two phases

$$E \simeq \frac{Z'_2 U(r'_2) - Z_2 U(r_2)}{Z' - Z} \quad (2)$$

The task of identifying all plausible morphologies of our system is clearly more challenging than comparing them energetically. There is hardly any systematic way of doing this, which would go beyond an educated guess. Nevertheless, one can considerably limit the search by making a number of assumptions based on general principles [6]: (i) In order to avoid direct contacts of the same-type particles, the structures should be bipartite, i.e. they should consist of two sub-lattices corresponding to the two types of particles, so that all the nearest neighbors were of opposite types. (ii) All the nearest neighbors should have the same bond length. This is needed to take advantage of the cohesive energy, as long as we model the particles as rigid sticky spheres. (iii) The structure is likely to possess a high symmetry: we consider only crystalline morphologies, with all equivalent sites. The violations of this criterium are fairly rare (e.g. quasicrystals).

In the table below, the candidate phases satisfying the above principles are classified accordingly to their coordination numbers and the space dimensionality.

Z	2D	3D
3	Honeycomb	Gyroid
4	Square (SQ)	Diamond (D)
5		Honeycomb Stacking (HS)
6		Simple Cubic (SC)
8		Body-Centered Cubic (BCC)

Note that in the limit of large aspect ratio, among various phases with the same Z , the one with the largest r_2 is energetically preferred, independently on the number of the second nearest neighbors (Z_2). Likewise, since r_2 goes down with the increase of coordination number, Z , the transition value of E , given by Eq. (2), asymptotically reaches value $Z_2 U(r_2)$, determined by the parameters (Z_2, r_2) of the higher- Z phase. In other words, the higher Z , the higher is the parameter $E(Z)$ of the transition between Z - and $Z + 1$ -coordinated phases. One can conclude that the sequence of the phases in the large aspect ratio regime is generic and should be independent of the particular choice of the repulsive potential: BCC($Z = 8$)–SC($Z = 6$)–Honeycomb Stacking ($Z = 5$)–Diamond($Z = 4$). The possibility of the self-assembly of the diamond lattice is especially exciting, because of its potential as a photonic bad gap structure [2].

The energetic difference between the two $Z = 3$ phases in the above table is only due to interactions of the third-nearest neighbors, which makes it irrelevant for a realistic situation. Unless the system is confined to 2D, this suggests that the observed morphology with $Z = 3$ will typically be a disordered one. There is no true phase transitions for ($Z < 3$) because of the low dimensionality of the dominant structures.

As the aspect ratio D/ξ is being decreased, one can expect two types of events: (i) "squeezing out" of certain phases by their neighbors; (ii) replacing one structure with another without changing Z . As one can see from Figure 1(a), the phase diagram obtained for exponential potential, $U(r) = U_0 \exp(-(r - d)/\xi)$ provides examples of the both kinds. One of them is particularly striking: at certain aspect ratio, the system undergoes a transition from 3D diamond lattice to 2D membrane with in-plane square order. Even though this order is known to be strongly affected by long-range fluctuations [3], the corresponding Landau-Pierls effect does not have any divergent contributions to the chemical potential of the 2D phase. One may refer to **D** – **SQ** transition as *spontaneous compactification*. Although the found 2D phase is somewhat similar to lipid membranes, it is built by particles with isotropic effective interactions (unlike lipids). The same holds for the diamond lattice: unlike the diamond structures in nature, in our case it is due to the competition of relatively simple *isotropic* potentials!

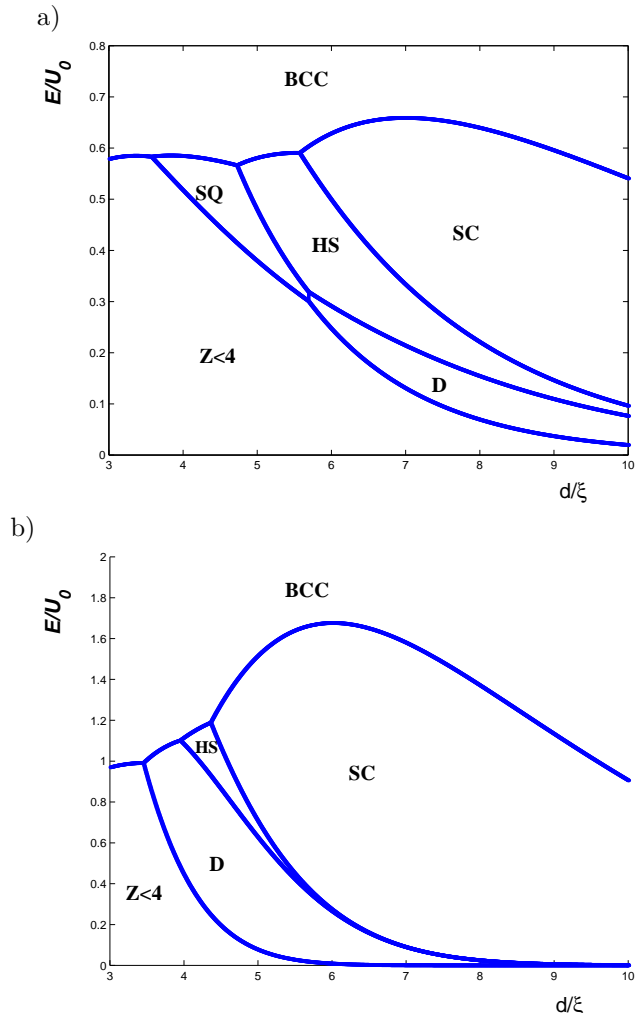


FIG. 1. Calculated phase diagram of the system for exponential (a) and Gaussian (b) forms of the repulsive potential $U(r)$.

As it was argued, the major features of the obtained phase diagram are fairly independent of the choice of the form of the inter-particle potential. To check this, we have calculated the phase diagram for two types of interactions, exponential and Gaussian, $U(r) = \exp(-(r - d)^2/2\xi^2)$ (see Figure 1). The major difference is that the square lattice (**SQ**) completely disappears in the Gaussian case. In addition the diamond lattice (**D**) significantly expands at the expense of **SQ** and **HS** phases. This trend appears to be quite general: the balance between the two competing $Z = 4$ phases, **D** and **SQ**, shifts towards Diamond for potentials with a super-exponential decay, while the region of stability of **SQ** expands for sub-exponential $U(r)$ (such as power laws, stretched exponentials, or Yukawa interaction).

We now proceed with the discussion of a plausible experimental implementation of the proposed system. As we have already mentioned, type-dependent "DNA bridging" of colloidal particles is an appealing way to introduce the AB attraction. As to the repulsive inter-

actions, there are several candidates in the colloidal science. Unfortunately, using of electrostatic repulsion in our case is problematic: in order for it to be relevant, the salt concentration needs to be much lower than at the physiological conditions. As a result, there would be a high electrostatic barrier for DNA duplex formation.

An alternative way to introduce the soft-core repulsion is through steric interactions of polymer-covered particles. Here we focus on a particular scenario in which the repulsion is due to DNA molecules with only one “sticky end” (complementary to either A or B markers). Unlike linker DNA, these one-arm molecules do not result in bridging and play a role of a buffer. We will assume that both the buffer-DNA and the linkers are double stranded, with the exception of the short terminal segments. The strength of the interaction of these sticky ends with the complementary markers can be characterized by DNA concentration c_0 , at which the condensation would occur (i.e. when the chemical potential of an adsorbed chain would become equal to that in the solution). If the actual concentration of the buffer-DNA, c , is much lower than c_0 , the number of the adsorbed chains per particle is $N = N_{\max}c/c^{(0)}$. Here N_{\max} is the total number of markers per particle. For the sake of simplicity, we assume that N^{\max} and N are the same for A and B particles, i.e. $c_A/c_B = c_A^{(0)}/c_B^{(0)}$.

Note that we have totally neglected the excluded volume interactions between the DNA molecules, which might seriously decrease the coverage compared to our result. The reason for this is twofold. First, the optimal coverage (discussed below) corresponds to a moderate overlap between the adsorbed chains. Second, the high rigidity of a double-strand DNA molecule results in the excluded volume effects being negligible within a single chain as long as it remains shorter than several thousands persistence lengths, $l_p \simeq 50 \text{ nm}$. Thus, the adsorbed DNA molecules can be treated as phantom Gaussian chains, which only interact with hard surfaces of the particles, but not with each other. Since the adsorption is reversible, the confined chains are being “squeezed out” when the gap between two particles, $r - d_0$ becomes comparable to the gyration radius of the DNA chain, R_g . The corresponding energetic penalty can be calculated in the spirit of the Deryagin approximation [7] (from now on, we distinguish bare particle diameter, d_0 , and effective one, d):

$$U(r) \simeq 2NkT \frac{R_g}{d_0} \int_{(r-d_0)/R_g}^{\infty} \left[1 - \exp\left(-\frac{W(\Delta)}{kT}\right) \right] d\Delta \quad (3)$$

Here $W(\Delta)$ is the free energy penalty for the confinement of a Gaussian polymeric chain between two walls at separation $R_g\Delta$. It can be obtained by using the Schrödinger-like description of the ideal polymer [8,9]:

$$\frac{W(\Delta)}{kT} = \log \left(\frac{\sqrt{2/3}}{\Delta} \sum_{n=0}^{\infty} \exp \left[-\frac{1}{6} \left(\frac{\pi(1+2n)}{\Delta} \right)^2 \right] \right) \quad (4)$$

The resulting repulsive potential is shown on Figure 2.

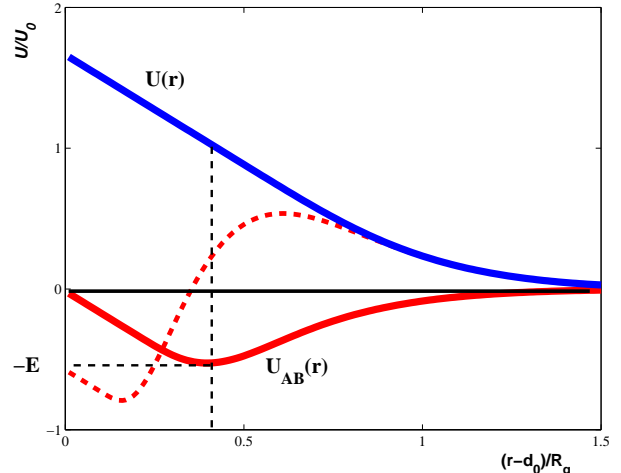


FIG. 2. Repulsive, $U(r)$, and attractive, $U_{AB}(r)$ potentials induced by DNA-particle interactions. Solid lines correspond to $R'_g/R_g = 1$. Note the barrier in the attractive potential for $R'_g/R_g = 0.5$ (dashed line).

The attractive potential induced by the linker-DNA can be calculated in a very similar manner. An important difference is that one has to take into account the elastic energy of a stretched linker, $W_{el}(\Delta) = 3kT\Delta^2/2$, and that the condensation concentration of the chains with two sticky ends is given by $c_{AB}^{(0)} = c_A^{(0)}c_B^{(0)}R_g^3$. Note that in a general case the gyration radius of a linker-DNA, R'_g , may be different from R_g .

$$U_{AB}(r) \simeq U(r) - \frac{2N_{\max}^2 kT c_{AB}}{3 c_{AB}^{(0)}} \left(\frac{R_g}{d_0} \right)^3 \times \int_{(r-d_0)/R_g}^{\infty} \exp \left[-\frac{W(\Delta) + W_{el}(\Delta)}{kT} \right] d\Delta \quad (5)$$

The relative strength of the attraction and the repulsion is controlled by the ratio of the concentrations of the buffer-DNA and linkers:

$$\frac{E}{U_0} = \frac{c_{AB}}{C_{AB}} - 1 \quad (6)$$

Here C_{AB} is the linker concentration at which E vanishes. For the case of $R'_g = R_g$,

$$C_{AB} \simeq \frac{3c_A^{(0)}c_B^{(0)}R_g^5}{N_{\max}d^2} \quad (7)$$

The absolute value of the energy scale in the problem is also controllable by concentration: according to Eq. (3),

$$U_0 \simeq NkT \frac{R_g}{d} \quad (8)$$

This scale should be of order of several kT to ensure that the phase diagram is not affected by the thermal fluctuations, and that the escape time from the potential well of depth $E \equiv -\min(U_{AB}(r))$ is not too long. By comparing Eqs. (7) and (8), we conclude that $C_{AB} \simeq c_A c_B R_g^6 / d^3$.

As one might expect, the tail of repulsive potential $U(r)$ is well described by a Gaussian with the characteristic length scale $\xi \simeq R_g$:

$$U(r) \sim \exp \left[-\frac{3}{2} \left(\frac{r-d}{R_g} + \beta \right)^2 \right]. \quad (9)$$

Here d is the effective diameter which is determined by the position of the minimum of $U_{AB}(r)$, and the bias $\beta \simeq 0.15 + (d - d_0)/R_g$. For the case $R'_g/R_g = 1$, shown on Figure 2, $\beta \simeq 0.6$. Thus, the corresponding phase diagram should be somewhere halfway between the Gaussian and exponential ones. By increasing the ratio R'_g/R_g one can move the system more towards exponential regime, because the position of the minimum changes roughly linearly with the radius of the linker DNA. However, the dynamic range of R'_g/R_g is rather limited: the long linkers would result in the additional attraction beyond the nearest neighbors, which would violate our initial assumptions.

In the opposite regime, $R'_g < R_g$, the particles need to overcome a significant energetic barrier before they start feeling the attraction (see Figure 2). The existence of this barrier is the major reason why we suggest to use linkers of at least several persistence lengths. In this case, the above Gaussian description may be applied. As we have shown, when the gyration radius of the linkers matches the scale of the repulsive potential, the particles may create a bound state without the need of overcoming any barrier. Thus, if the linkers are double-strand DNA molecules, the minimal value of $\xi_{\min} \sim l_p \sim 100nm$.

The fundamental time scale of the problem is set by the lifetime of the AB contact, which can be estimated as

$$\tau \simeq \frac{\eta d R_g^2}{kT} \exp \left(\frac{E}{kT} \right). \quad (10)$$

Here η is the solvent viscosity, and we have assumed that the trial frequency is limited by the particle diffusion rather than by the departure rate of a linker–DNA. Since this desorption rate can be estimated as $kT c_{AB}^{(0)} / \eta$, our regime requires $c_{AB}^{(0)} > R_g'^{-3}$. This corresponds to a moderate marker–linker affinity, $\epsilon/kT < 3 \log(R_g/a) \simeq 20$ (here $a \sim 0.1nm$ is the microscopic scale defined by the rigidity of hydrogen bonding between complementary DNA threads).

Since the relaxation time (10) grows fast with the linker scales of the problem, the optimal regime corresponds to minimal value of $R_g \simeq \xi_{\min} \simeq .1\mu m$, i.e $d \sim 1\mu m$. Within the assumption that the DNA–based key–lock complex would remain functional up to the coverage of 1 marker molecule per $\sim 10nm^2$, $N_{\max} \sim 10^4$. According to Eqs. (7-8), this yields $c_A/c_A^{(0)} = c_B/c_B^{(0)} \sim 10^{-3}$, and $c_{AB}/c_{AB}^{(0)} \sim 10^{-5}$. The fundamental time scale (10) at the optimal regime is less than a minute. However, the true relaxation time of the system is determined by slow aggregation and growth processes. Hopefully, they both can be facilitated by using a commensurate substrate.

Now that we have identified the optimal regime and interpreted the control parameters of the phase diagram in terms of the experimental ones, we should also determine how damaging is disorder for the expected behavior. The effect of the particle polydispersity is likely to be similar to the one in conventional colloidal self–assembly. The new effect is that the interactions are due to DNA chains, whose number per contact is of order of 1. Nevertheless, because of the reversibility of DNA–particle contact, the time–averaged interaction free energy varies only due to the discreteness of the markers. The corresponding disorder can be estimated as $\delta E/U_0 \simeq R_g \sqrt{N_{\max}}/d < 0.1$. As one can see from Figure 1, such a variation of E/U_0 is tolerated in this problem, especially for the Gaussian potential.

Acknowledgement The author is grateful to P. Wiltzius, C. Henley, B. Shraiman, and Z. Chen for the useful discussions and valuable information.

-
- [1] P. Pieranski, *Phys. Rev. Lett.*, **45**, 569 (1980); A. E. Larsen and D. G. Grier *Phys. Rev. Lett.* **76**, 3862 (1996); J. X. Zhu, M. Li, R. Rogers, W. Meyer, R. H. Ottewill, W. B. Russell, P. M. Chaikin, *Nature* **387**, 883 (1997).
 - [2] S. Fan, P. R. Villeneuve, and J. D. Joannopoulos, *Phys. Rev. B*, **54**, 11245 (1996); D. F. Sievenpiper, M. E. Sickmiller, and E. Yablonovitch, *Phys. Rev. Lett.* **76**, 2480 (1996).
 - [3] P. M. Chaikin and T. C. Lubensky, *Principles of Condensed Matter Physics*, Cambridge Univ. Press., Cambridge, UK (2000).
 - [4] C. A. Mirkin, R. L. Letsinger, R. C. Mucic, J. J. Storhoff, *Nature*, **382**, 607 (1996); J. J. Storhoff, ; A. A. Lazarides, R. C. Mucic, C. A. Mirkin, R. L. Letsinger, G. C. Schatz, *J. Am. Chem. Soc.* **122**, 4640 (2000).
 - [5] J. J. Storhoff and C. A. Mirkin, *Chem. Rev.*, **99**, 1849 (1999).
 - [6] W.-J. Zhu and C. L. Henley, *Europhys. Lett.* **51**, 133 (2000); W.-J. Zhu and C. L. Henley, Preprint (2001).
 - [7] J. N. Israelashvili, *Intermolecular and Surface Forces* (Academic Press, London, 1985)
 - [8] P.-G. de Gennes, *Scaling Concepts of Polymer Physics*

(Cornell University Press, 1979).

- [9] A. Yu. Grosberg and A. R. Khokhlov, *Statistical Physics of Macromolecules* (AIP, New York, 1994).